Journal of Power Sources 180 (2008) 539–545

Contents lists available at ScienceDirect

Journal of Power Sources

journal homepage: www.elsevier.com/locate/jpowsour

Electrochemical AFM study of $LiMn_2O_4$ thin film electrodes exposed to elevated temperatures

Takayuki Doi[a,*], Minoru Inaba[b], Hiroshi Tsuchiya[c], Soon-Ki Jeong[d], Yasutoshi Iriyama[c], Takeshi Abe[c], Zempachi Ogumi[c]

[a] Institute for Materials Chemistry and Engineering, Kyushu University, 6-1 Kasuga-koen, Kasuga 816-8580, Japan
[b] Department of Molecular Science and Technology, Faculty of Engineering, Doshisha University, Kyotanabe, Kyoto 610-0321, Japan
[c] Department of Energy & Hydrocarbon Chemistry, Graduate School of Engineering, Kyoto University, Nishikyo-ku, Kyoto 615-8510, Japan
[d] Department of Chemical Engineering, Soonchunhyang University, Asan, Chungnam 336-745, Republic of Korea

ARTICLE INFO

Article history:
Received 23 January 2008
Received in revised form 21 February 2008
Accepted 21 February 2008
Available online 29 February 2008

Keywords:
Lithium-ion battery
Lithium manganese oxide
Capacity fading
Atomic force microscopy
Surface morphology

ABSTRACT

Surface morphology changes of $LiMn_2O_4$ thin film positive electrodes in lithium-ion batteries after repeated potential cycling or storage at elevated temperatures were observed by in situ atomic force microscopy (AFM) to elucidate the origin of capacity fading of $LiMn_2O_4$. After repeated potential cycling in the overall potential range from 3.50 to 4.30 V at elevated temperatures, the entire thin film surface was covered with small round-shaped particles accompanied by capacity fading of the electrode, while no significant changes were observed at 25 °C. The discharge capacity decreased more significantly when cycled in the lower potential range (3.81–4.07 V) than when cycled in the higher potential range (4.04–4.30 V). After storage at elevated temperatures at a depth of discharge (DOD) of 75%, which is located in the lower potential range, similar surface morphology changes were observed. In addition, discharge capacity markedly decreased, and the crystallinity of the $LiMn_2O_4$ thin film was lowered after storage. Hence, the observed changes in morphology at elevated temperatures are closely related to capacity fading of the $LiMn_2O_4$ thin film. The loss of crystallinity was caused by the formation of small particles on the $LiMn_2O_4$ surface, which would be accelerated on the $LiMn_2O_4$ surface in contact with an electrolyte solution through some kind of dissolution/precipitation reaction.

1. Introduction

The interface between an electrode and an electrolyte plays a very important role as a reaction field for lithium-ion transfer in lithium-ion batteries. Electrochemical lithium-ion insertion and extraction reactions take place at negative and positive electrodes, respectively, during charging, and *vice versa* during discharging in lithium-ion batteries [1] Ideally, the electrode reactions should proceed reversibly during repeated charge and discharge cycles. In practice, however, considerable experimental evidence shows that irreversible reactions, such as surface film formation accompanied by electrolyte decomposition and deterioration of host structure of electrode materials, occur over repeated cycling [2,3]. Because of the high energy densities of lithium-ion batteries, they are expected as possible power sources in hybrid electric vehicles. However, before lithium-ion batteries can be used in high-power applications, their performance still needs to be improved with regard to battery cycle life, rate capability, and safety. Because irreversible reactions result in performance degradation of lithium-ion batteries, they should be minimized to extend the battery cycle life.

Spinel $LiMn_2O_4$ has an isotropic structure, which provides a three-dimensional network for lithium ions to diffuse easily [4,5]. This feature is advantageous for rapid charge/discharge reactions. Hence, $LiMn_2O_4$ is a possible candidate for use as a positive electrode in lithium-ion batteries for high-power applications. However, spinel $LiMn_2O_4$ has a drawback: the capacity fades rapidly during charge/discharge cycling and storage, particularly at a specific depth of discharge (DOD) at elevated temperatures. Several possible mechanisms for this capacity fading of spinel $LiMn_2O_4$ have been proposed, which include electrolyte decomposition at high potentials, slow dissolution of $LiMn_2O_4$ through a disproportionation reaction, an irreversible structural transition due to the Jahn-Teller distortion, and transformation of the unstable two-phase structure at a higher potential region to a more stable single-phase structure via the loss of MnO and Mn_2O_3 [6–8]. Although all of these factors are related with the capacity fading of $LiMn_2O_4$ to some extent, the primary cause has not yet been clarified.

* Corresponding author. Tel.: +81 92 583 7657; fax: +81 92 583 7791.
E-mail address: doi@cm.kyushu-u.ac.jp (T. Doi).

0378-7753/$ – see front matter © 2008 Elsevier B.V. All rights reserved.
doi:10.1016/j.jpowsour.2008.02.054

In situ scanning probe microscopy (SPM) techniques, such as scanning tunneling microscopy (STM) and atomic force microscopy (AFM), have been recently applied to the analysis of electrode surface reactions in lithium-ion batteries because it is possible to observe directly changes in surface morphology in liquid electrolyte solutions. The authors previously reported the changes in surface morphology of $LiMn_2O_4$ thin film electrodes after repeated potential cycling at room temperature [9,10], in which we used STM. In the present study, morphology changes of $LiMn_2O_4$ thin film electrodes after storage at various DODs at elevated temperatures were investigated. We used AFM in the present study because non-conductive products may be formed on the surface. The effects of storage on charge and discharge characteristics were also investigated, and the correlation between capacity fading and changes in the surface morphology is discussed.

2. Experimental

$LiMn_2O_4$ thin films were deposited on Pt substrates by pulsed laser deposition (PLD). A KrF excimer laser (Japan Storage Batteries, Model EXL-210) was used as a light source. The substrate temperature was kept at 700 °C, which was by 100 °C higher than that in our previous work [5,9,10], to obtain highly crystallized $LiMn_2O_4$ thin films. A target consisting of a sintered Li–Mn–O pellet with a lithium-excess ratio of (Li/Mn) = 0.7 was irradiated with the laser beam through a SiO_2 glass window under an oxygen atmosphere of 27 Pa. The base pressure of the vacuum chamber was $<1 \times 10^{-6}$ Pa. The energy fluence of the beam was set at 1.5 J cm^{-2} with a repetition frequency of 10 Hz. After deposition for 1 or 2 h, the substrate was cooled to room temperature at 2.1 °C min^{-1} under an oxygen atmosphere. Further details of the procedure were described previously [9]. The thin films obtained by PLD were characterized by X-ray diffraction (XRD) (Rigaku, Rint2200) equipped with a graphite monochromator with a scintillation detector. Typical working conditions were 50 kV and 300 mA with a scanning speed of 0.6° min^{-1}. The total mass and the Li/Mn ratio of the thin films were determined by inductively coupled plasma (ICP) spectroscopy (Shimadzu, ICP-1000II).

The electrochemical properties of the thin films were studied by cyclic voltammetry and charge and discharge tests using a three-electrode cell. The effective electrode surface area was limited to 0.48 cm^2 by an O-ring. Both the reference and the counter electrodes were lithium metal. The electrolyte solution was 1 mol dm^{-3} $LiPF_6$ dissolved in propylene carbonate (PC) (Kishida Chemical Co. Ltd., Battery grade). Cyclic voltammetry was carried out repeatedly at a scan rate of 1 mV s^{-1} within a given potential range at 25, 60, or 80 °C using a potentiostat/galvanostat (EG&G PAR, model 273A). The influence of storage at different DODs at elevated temperature on charge and discharge characteristics was investigated in the following manner. After an initial potential cycle between 3.50 and 4.30 V, the electrode was swept to a given potential and held at that potential. The temperature of the cell was then raised to a given temperature. After being maintained at that temperature for a given time, cyclic voltammetry was carried out between 3.50 and 4.30 V.

In situ AFM observation coupled with cyclic voltammetry and potentiostatic polarization was carried out with an AFM system (Molecular Imaging, PicoSPM) equipped with a potentiostat (Molecular Imaging, PicoStat) and a laboratory-made electrochemical cell. AFM images were obtained in the contact mode with a microcantilever made of silicon nitride (spring constant 0.02 N m^{-1}). The geometric surface area of the $LiMn_2O_4$ thin film was limited to 1.2 cm^2 by an O-ring. Both the reference and the counter electrodes were lithium metal. The electrolyte used was 1 mol dm^{-3} $LiPF_6$/PC. More details on the configuration of the electrochemical AFM cell were described previously [11,12]. To observe changes in the surface morphology that occurred during the preceding potential cycle, AFM images were obtained at a sample potential of 3.50 V at 25 °C after potential cycling between 3.50 and 4.30 V at a sweep rate of 1 mV s^{-1} at 25 or 60 °C. This procedure was repeated up to the 90th potential cycle. In addition, the influence of DOD on changes in surface morphology was investigated in the following manner. After a potential cycle between 3.50 and 4.30 V at room temperature of ca. 25 °C, the electrode was swept to a given potential and kept at that potential. The temperature of the cell was then raised to 80 °C. After storage for a given time, the cell was cooled to room temperature to observe the surface morphology by AFM. All electrochemical and AFM measurements were carried out in an argon glove box (Miwa, MDB-1B + MM3-P60S) with a dew point below −60 °C.

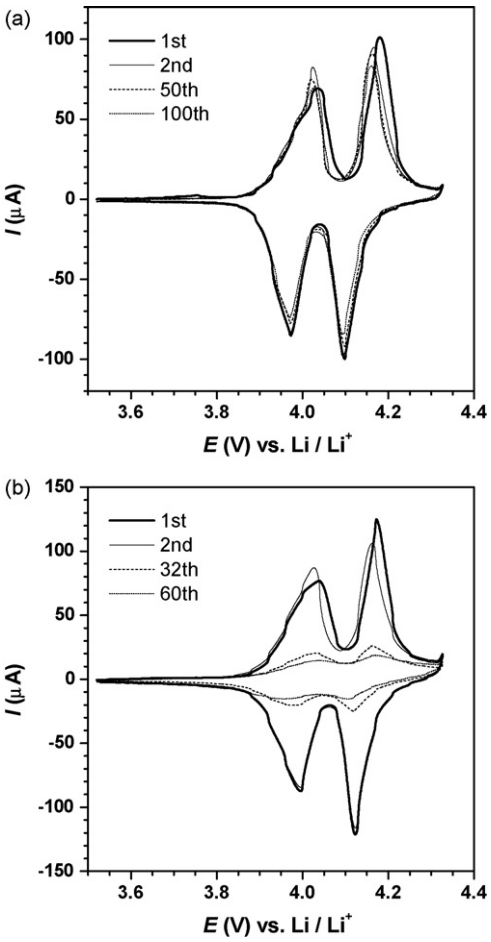

Fig. 1. Cyclic voltammograms of $LiMn_2O_4$ thin films (ca. 100 nm) between 3.50 and 4.30 V in 1 mol dm^{-3} $LiPF_6$/PC at (a) 25 and (b) 60 °C. Scan rate was 1 mV s^{-1}.

3. Results and discussion

The XRD pattern of the resultant thin film, which is shown in Fig. 8a for later discussion, indicated that single-phase spinel $LiMn_2O_4$ was obtained; the peaks at 2θ angles of 18.6, 35.9, 37.7, 43.8, 48.0, 58.0, and 63.6° correspond to the (1 1 1), (3 1 1), (2 2 2), (4 0 0), (3 3 1), (5 1 1), and (4 4 0) diffraction lines, respectively. The lattice constant of the thin film was evaluated by a least-squares method to be 8.25 Å. ICP measurements showed that the Li/Mn atomic ratio of the thin film was 0.505. These results indicate that nearly stoichiometric spinel $LiMn_2O_4$ thin

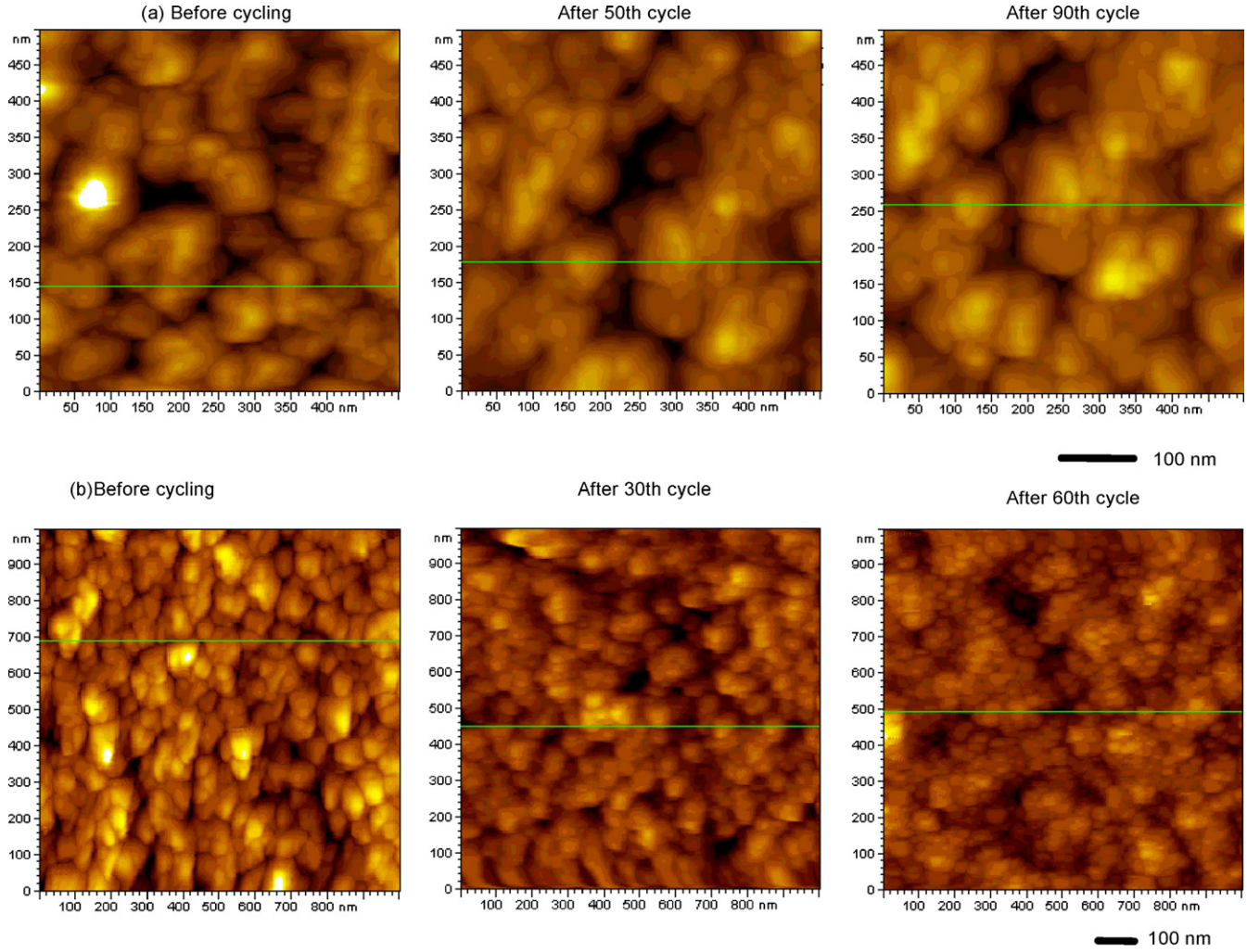

Fig. 2. AFM images of a $LiMn_2O_4$ thin film obtained (a) before cycling, after 50th and 90th cycle at 25 °C (500 nm × 500 nm), and (b) before cycling, after 30th and 60th cycle at 60 °C (1 μm × 1 μm) between 3.50 and 4.30 V in 1 mol dm^{-3} $LiPF_6$/PC.

films were obtained in this work. The thicknesses of the thin films were about 100 and 200 nm after deposition for 1 and 2 h, respectively.

Fig. 1 shows cyclic voltammograms of the $LiMn_2O_4$ thin films (ca. 100 nm) between 3.50 and 4.30 V at 25 and 60 °C. In each voltammogram, two pairs of redox peaks were clearly seen at ca. 4.0 and 4.1 V, which are characteristic of spinel $LiMn_2O_4$. In the voltammograms obtained at 25 °C, almost no change in peak potential was seen after repeated cycling, while a slight decrease in peak current was observed at the 100th cycle. These results were quite different from the results in our previous work; the redox peaks for a stoichiometric $LiMn_2O_4$ thin film prepared at 873 K by PLD broadened after repeated cycling in 1 mol dm^{-3} $LiClO_4$/PC [9,10]. This is probably caused by the difference in crystallinity of the thin films and/or in oxidative resistance of the electrolytes. On the other hand, substantial changes were observed in the voltammograms obtained at 60 °C; the peak currents decreased markedly, and the peak separation increased after repeated cycling. Based on our previous results that changes in the surface morphology of a $LiMn_2O_4$ thin film electrode are closely related to the capacity fading of the electrode, obvious changes in the morphology should have occurred during potential cycling at 60 °C [9,10]. Fig. 2 shows the changes in surface morphology of the $LiMn_2O_4$ thin film electrodes after potential cycling between 3.50 and 4.30 V at 25 and 60 °C. Both films consisted mostly of grains of about 80–100 nm in diameter before potential cycling. There was no change before and after just soaking in the electrolyte solution. In Fig. 2a (500 nm × 500 nm), no significant changes were observed even after the 90th cycle at 25 °C. We previously reported that small particles of around 120–250 nm appeared after the 20th cycle when a stoichiometric $LiMn_2O_4$ thin film was cycled between 3.5 and 4.25 V [9]. However, such newly formed particles could not be observed in Fig. 2a. On the other hand, the surface morphology significantly changed at 60 °C, as shown in Fig. 2b (1 μm × 1 μm); the entire surface was covered with small round-shaped particles about 20 nm in diameter after the 30th cycle. In addition, the surface became smoother after the 60th cycle, whereas steep valleys with a vertical interval of around 150 nm were seen in the height profiles before cycling. We previously reported that decomposition products of the solvents on a highly oriented pyrolytic graphite (HOPG) negative electrode could be mechanically removed by scanning repeatedly with the AFM tip [11,12]. However, this was not the case in the present study: no change in the surface morphology was observed after repeated scanning. Hence, the newly formed small particles did not consist of soft organic deposits, but of Li–Mn–O particles. These results suggest that the observed changes in morphology at 60 °C are closely related to the capacity fading of the $LiMn_2O_4$ thin film shown in Fig. 1.

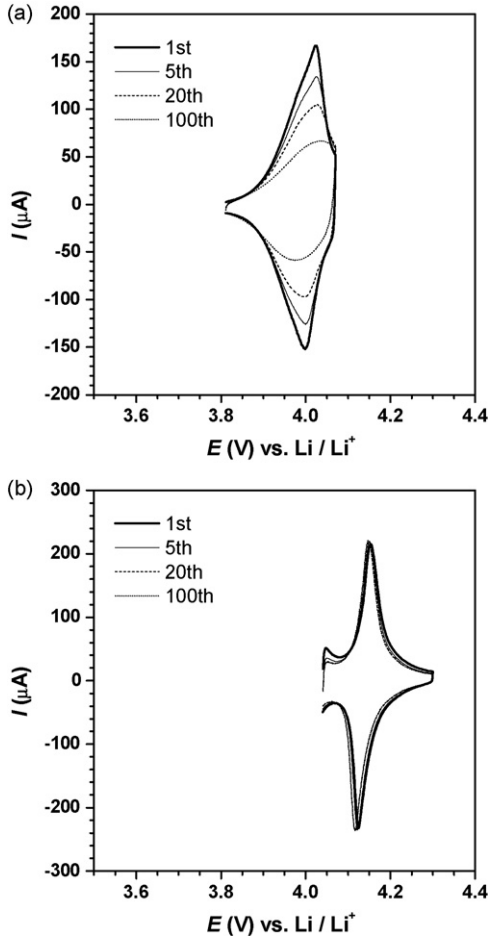

Fig. 3. Cyclic voltammograms of $LiMn_2O_4$ thin films (ca. 200 nm) between (a) 3.81 and 4.07 V and (b) 4.04 and 4.30 V in 1 mol dm^{-3} $LiPF_6$/PC at 80 °C. Scan rate was 1 mV s^{-1}.

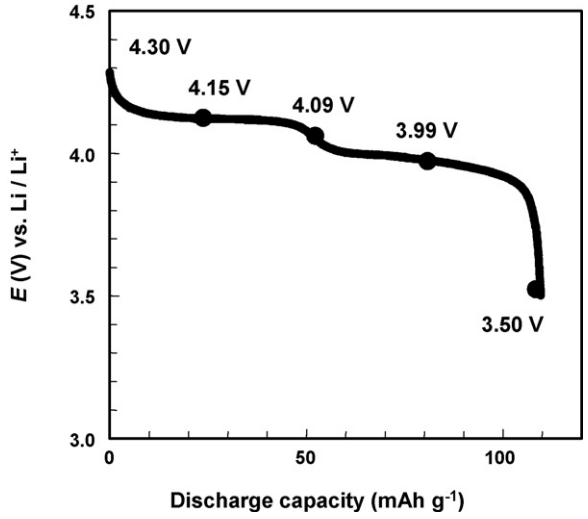

Fig. 4. A discharge curve of a $LiMn_2O_4$ thin film in 1 mol dm^{-3} $LiPF_6$/PC.

Cyclic voltammetry was carried out in different potential ranges to identify which potential range decreases the reversible capacity more significantly. Fig. 3 compares cyclic voltammograms of the $LiMn_2O_4$ thin films (ca. 200 nm) between 3.81 and 4.07 V, and between 4.04 and 4.30 V at 80 °C. A couple of redox peaks, which are due to the insertion or extraction of lithium ions at $LiMn_2O_4$, were seen in each voltammogram. The discharge capacity, which was estimated from the area of the reduction peak, retained 96% of the initial capacity at the 100th cycle in the higher potential range. On the other hand, it faded by 43% at the 100th cycle in the lower potential range and the peak separation gradually increased with repeated cycling. Thus, the redox peak current decreased more significantly when cycled in the lower potential range than when cycled in the higher potential range. Based on these results, potential cycling in the lower potential range seems to be responsible for the observed changes in morphology at 60 °C shown in Fig. 2.

The influence of DOD on capacity fading upon storage at elevated temperatures was investigated. Fig. 4 shows an initial discharge curve of the $LiMn_2O_4$ thin film. The $LiMn_2O_4$ thin film electrodes were stored at 80 °C at electrode potentials of 3.50, 3.99, 4.09, 4.15, and 4.30 V, which correspond to 100, 75, 50, 25, and 0% DOD, respectively. Fig. 5 shows cyclic voltammograms of the $LiMn_2O_4$ thin films (ca. 200 nm) after storage at 0, 25, 50, 75, and 100% DOD at 80 °C. At each DOD, the redox peaks broadened and the peak separation increased compared with those before storage. The most substantial changes were observed in the voltammograms after storage at 75% DOD; both pairs of the redox peaks in the higher and lower potential ranges almost disappeared after storage for 16 h. The variations of relative discharge capacities with time of storage are summarized in Fig. 6. The discharge capacities were evaluated by integrating the voltammograms and normalized by the initial capacity at each DOD. It is clear that the discharge capacity decreased most significantly after storage at 75% DOD. This tendency is very similar to results in the literature [13–15]. The discharge capacities decreased by 60% after storage at 75% DOD for 36 h. It should be noted that the observed drop of more than 60% in discharge capacity was much larger than those for micrometer-sized $LiMn_2O_4$ powders reported in the literature [16–18]. The thickness of the $LiMn_2O_4$ thin films used here was about 200 nm. The original grain size of $LiMn_2O_4$ was around 80–100 nm, and hence the majority of the grains were exposed to the surface of the thin film to organize an interface with an electrolyte solution. These facts suggest that the capacity fading is more serious for the surface of $LiMn_2O_4$ than for its interior. In other words, the $LiMn_2O_4$ surface in contact with an electrolyte should readily deteriorate during storage.

Fig. 7 shows changes in the morphology of the $LiMn_2O_4$ thin film after storage at 50, 75, and 100% DOD at 80 °C. Each film consisted mostly of grains of about 80–100 nm in diameter before potential cycling. Their size remained almost unchanged up to 24 h of storage at 50 and 100% DODs, as shown in Fig. 7a and c. Almost the same tendency was obtained after storage at 0 and 25% DODs. On the other hand, the original grains of $LiMn_2O_4$ clearly became smaller after storage at 75% DOD for 4 h, as shown in Fig. 7b; small particles of around 20–30 nm appeared and the entire surface was covered with them. The small particles were very similar to those observed after repeated cycling between 3.50 and 4.30 V at 60 °C shown in Fig. 2b. These results indicate that the capacity fading at 75% DOD is closely related to the observed changes in morphology.

It is widely known that manganese ions in spinel $LiMn_2O_4$ readily dissolve in electrolyte solutions, particularly at the fully charged state (0% DOD, λ-MnO_2) [13,14]. On the other hand, capacity fading occurs most significantly after storage at 75% DOD at elevated temperatures. Hence, the capacity fading cannot be explained simply by dissolution of manganese ions. Li et al. reported a structural anomaly in the composition range of $0.6 < x < 1$ in $Li_xMn_2O_4$, especially in the vicinity of $x = 0.75$. They observed the co-existence of two metastable phases (phases A and B) for their $Li_xMn_2O_4$ sam-

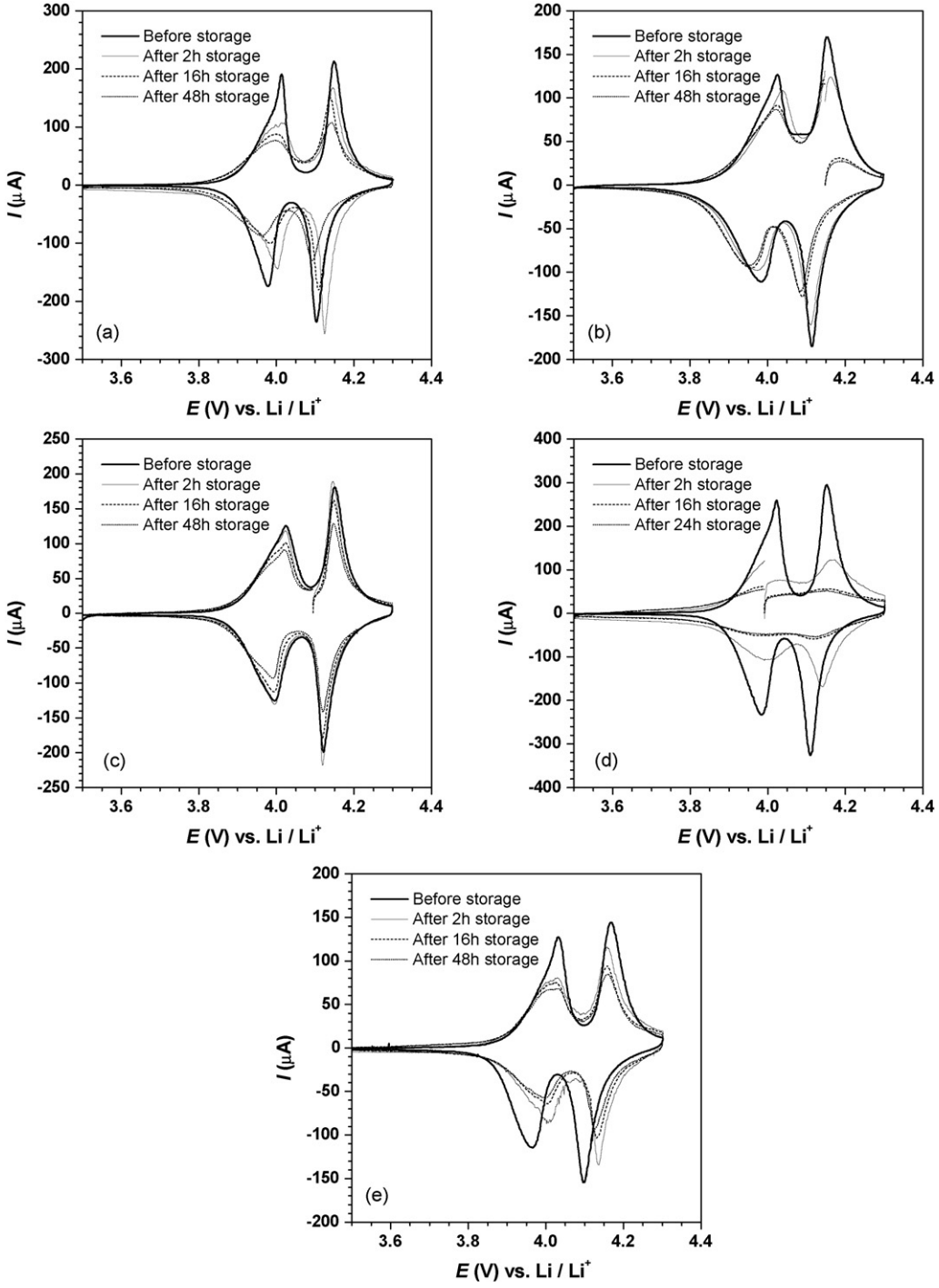

Fig. 5. Cyclic voltammograms of $LiMn_2O_4$ thin films (ca. 200 nm) after storage at (a) 0%, (b) 25%, (c) 50%, (d) 75%, and (e) 100% DOD in 1 mol dm^{-3} $LiPF_6$/PC at 80 °C. Scan rate was 1 mV s^{-1}.

ples synthesized by reacting LiI and λ-MnO_2 [19]. These two phases changed into a single stable phase at room temperature, which showed that they were metastable phases formed by a kinetic limitation. On the other hand, one of the two phases, which has a larger lattice constant (phase A), disappeared gradually on keeping the $Li_xMn_2O_4$ electrode at $x = 0.75$ at 80 °C [20]. These results indicate that phase A should become amorphous and/or be dissolved into an electrolyte to disappear during storage at 80 °C. Based on their results and the morphology changes observed after storage at 75% DOD in Fig. 7 in this work, amorphous Li–Mn–O with small particle sizes would be newly formed after storage at 80 °C through some kind of dissolution/precipitation reactions in the vicinity of the electrode surface, as we suggested previously [9]. Fig. 8 compares XRD patterns of the $LiMn_2O_4$ thin film electrodes before and after storage at 75% DOD at 80 °C for 4 h. Although no new peak appeared after storage, the full width at half-maximum of the peaks assigned to $LiMn_2O_4$ broadened by a factor of 1.2 times. The peak broadening is attributable to the newly generated small particles, which proves the assumption mentioned above. The capacity fading was much more serious for the $LiMn_2O_4$ thin film than for micron-sized $LiMn_2O_4$ powders, as described earlier. Hence, such a loss of crystallinity would be accelerated on the $LiMn_2O_4$ surface in contact with an electrolyte solution through the formation of small particles.

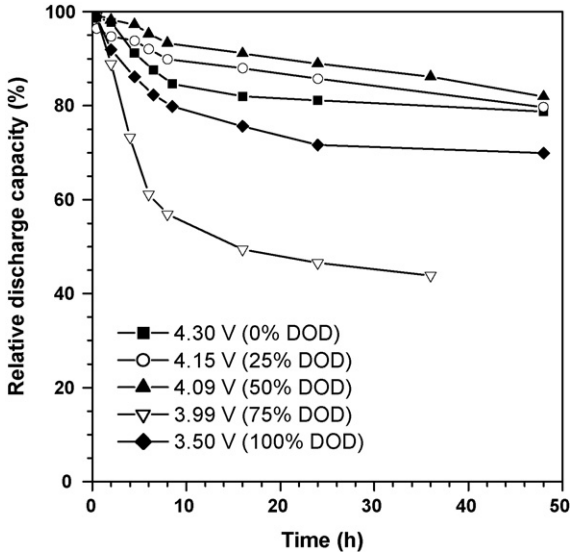

Fig. 6. Variation of relative discharge capacities of $LiMn_2O_4$ thin films with time of storage at 0, 25, 50, 75, and 100% DOD in 1 mol dm^{-3} $LiPF_6$/PC at 80 °C.

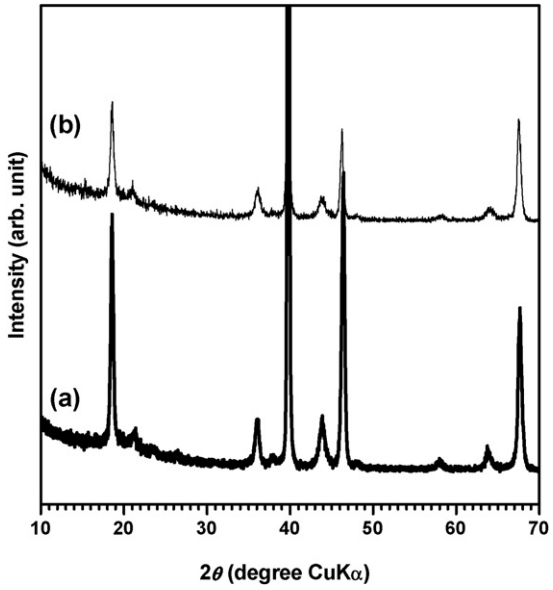

Fig. 8. X-ray diffraction patterns of $LiMn_2O_4$ thin films obtained (a) before and (b) after 4 h storage at 75% DOD in 1 mol dm^{-3} $LiPF_6$/PC at 80 °C.

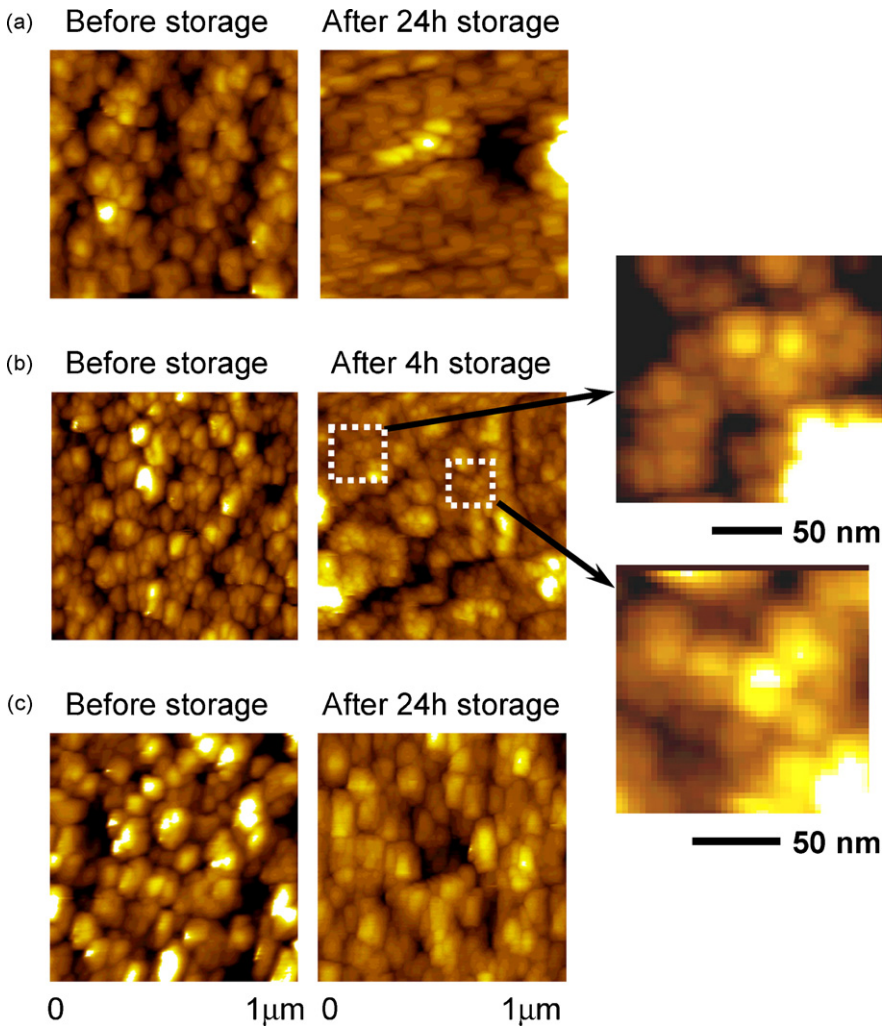

Fig. 7. AFM images 1 μm × 1 μm of $LiMn_2O_4$ thin films obtained before and after storage at (a) 50%, (b) 75%, and (c) 100% DOD in 1 mol dm^{-3} $LiPF_6$/PC at 80 °C.

4. Conclusions

Nearly stoichiometric $LiMn_2O_4$ thin film positive electrodes were prepared by PLD. Surface morphology changes of the films after repeated potential cycling or storage at elevated temperatures were investigated in 1 mol dm^{-3} $LiPF_6$/PC by in situ AFM observations, and were correlated with capacity fading of $LiMn_2O_4$. The entire thin film surface was covered with small round-shaped particles about 20 nm after repeated potential cycling between 3.50 and 4.30 V at elevated temperatures. The observed changes in morphology are closely related to the capacity fading of the $LiMn_2O_4$ thin films at elevated temperatures. The discharge capacity decreased more significantly when cycled in the lower potential range (3.81–4.07 V) than when cycled in the higher potential range (4.04–4.30 V). Hence, potential cycling in the lower potential range was responsible for the observed changes in morphology.

The influence of DOD on capacity fading upon storage at elevated temperatures was also investigated. The discharge capacity decreased most significantly at 75% DOD after storage at 80 °C. The drop in discharge capacity was much larger than those for micrometer-sized $LiMn_2O_4$ powders reported in the literature, which suggested that the capacity fading is more serious for the surface of $LiMn_2O_4$ in contact with electrolyte solution than for its interior. The entire thin film surface was covered with small round-shaped particles about 20–30 nm after storage at 75% DOD, which was very similar to those observed after repeated cycling between 3.50 and 4.30 V at elevated temperatures. In addition, the crystallinity of the $LiMn_2O_4$ thin film was lowered after storage. Based on these results, the observed changes in morphology at elevated temperatures are closely related to capacity fading of the $LiMn_2O_4$ thin film. The loss of crystallinity was caused by the formation of small particles on the $LiMn_2O_4$ surface, which would be accelerated on the $LiMn_2O_4$ surface in contact with an electrolyte solution through some kind of dissolution/precipitation reaction. These deterioration phenomena observed for the $LiMn_2O_4$ thin film electrodes are attributable to the appearance of metastable two phases of $Li_xMn_2O_4$ at 75% DOD at elevated temperatures as reported in the literature. Hence, phase stability of $Li_xMn_2O_4$ is essential to achieve highly reversible charge and discharge reactions at elevated temperatures.

References

[1] M. Winter, J.O. Besenhard, M.E. Spahr, P. Novák, Adv. Mater. 10 (1998) 725.
[2] M. Inaba, Z. Siroma, A. Funabiki, Z. Ogumi, T. Abe, Y. Mizutani, M. Asano, Langumir 12 (1996) 1535.
[3] D. Aurbach, J. Power Sources 89 (2000) 206.
[4] T. Ohzuku, M. Kitagawa, T. Hirai, J. Electrochem. Soc. 137 (1990) 769.
[5] I. Yamada, T. Abe, Y. Iriyama, Z. Ogumi, Electrochem. Commun. 5 (2003) 502.
[6] R.J. Gummow, A. de Kock, M.M. Thackeray, Solid State Ionics 69 (1994) 59.
[7] M.M. Thackeray, Y.S. Horn, A.J. Kahaian, K.D. Kepler, E. Skinner, J.T. Vaughey, S.A. Hackney, Electrochem. Solid-State Lett. 1 (1998) 7.
[8] Y. Xia, Y. Zhou, M.J. Yoshio, J. Electrochem. Soc. 144 (1997) 2593.
[9] M. Inaba, T. Doi, Y. Iriyama, T. Abe, Z. Ogumi, J. Power Sources 81/82 (1999) 554.
[10] T. Doi, M. Inaba, Y. Iriyama, T. Abe, Z. Ogumi, J. Electrochem. Soc. 155 (2008) A20.
[11] S.-K. Jeong, M. Inaba, T. Abe, Z. Ogumi, J. Electrochem. Soc. 148 (2001) A989.
[12] M. Inaba, H. Tomiyasu, A. Tasaka, S.-K. Jeong, Z. Ogumi, Langmuir 20 (2004) 1348.
[13] M. Saitoh, M. Sano, M. Fujita, M. Sakata, M. Takata, E. Nishibori, J. Electrochem. Soc. 151 (2004) A17.
[14] K. Takahashi, M. Saitoh, N. Asakura, T. Hibino, M. Sano, M. Fujita, K. Kifune, J. Power Sources 136 (2004) 115.
[15] Y. Shin, A. Manthiram, Chem. Mater. 15 (2003) 2954.
[16] R. Yazami, Y. Ozawa, J. Power Sources 153 (2006) 251.
[17] A. Manthiram, W. Choi, Electrochem. Solid-State Lett. 10 (2007) A228.
[18] H. Yamane, M. Saitoh, M. Sano, M. Fujita, M. Sakata, M. Takada, E. Nishibori, N. Tanaka, J. Electrochem. Soc. 149 (2002) A1514.
[19] G. Li, A. Yamada, Y. Fukushima, K. Yamaura, T. Saito, T. Endo, H. Azuma, K. Sekai, Y. Nishi, Solid State Ionics 130 (2000) 221.
[20] G. Li, Y. Iijima, Y. Kudo, H. Azuma, Solid State Ionics 146 (2002) 55.